Free Radical Biology and Medicine 89 (2015) 419–430

Contents lists available at ScienceDirect

Free Radical Biology and Medicine

journal homepage: www.elsevier.com/locate/freeradbiomed

Original Contribution

NOX4-dependent Hydrogen peroxide promotes shear stress-induced SHP2 sulfenylation and eNOS activation

Francisco J. Sánchez-Gómez [a], Enrique Calvo [b], Rosa Bretón-Romero [a], Marta Fierro-Fernández [a], Narayana Anilkumar [c], Ajay M. Shah [c], Katrin Schröder [d], Ralf P. Brandes [d], Jesús Vázquez [b], Santiago Lamas [a,*]

[a] Centro de Biología Molecular "Severo Ochoa" CSIC–UAM, Campus Universidad Autónoma, E-28049 Madrid, Spain
[b] Laboratory of Cardiovascular Proteomics, Centro Nacional de Investigaciones Cardiovasculares, 28029 Madrid, Spain
[c] Cardiovascular Division, British Heart Foundation Centre of Research Excellence, King's College London, London SE5 9NU, UK
[d] Vascular Research Centre, Institute for Cardiovascular Physiology, Goethe University, 60590 Frankfurt am Main, Germany

ARTICLE INFO

Article history:
Received 14 April 2015
Received in revised form
7 August 2015
Accepted 25 August 2015
Available online 30 September 2015

Keywords:
Endothelium
Laminar shear stress
Hydrogen peroxide
Sulfenylation
Redox signaling
Vasodilation
Free radicals

ABSTRACT

Laminar shear stress (LSS) triggers signals that ultimately result in atheroprotection and vasodilatation. Early responses are related to the activation of specific signaling cascades. We investigated the participation of redox-mediated modifications and in particular the role of hydrogen peroxide (H_2O_2) in the sulfenylation of redox-sensitive phosphatases. Exposure of vascular endothelial cells to short periods of LSS (12 dyn/cm^2) resulted in the generation of superoxide radical anion as detected by the formation of 2-hydroxyethidium by HPLC and its subsequent conversion to H_2O_2, which was corroborated by the increase in the fluorescence of the specific peroxide sensor HyPer. By using biotinylated dimedone we detected increased total protein sulfenylation in the bovine proteome, which was dependent on NADPH oxidase 4 (NOX4)-mediated generation of peroxide. Mass spectrometry analysis allowed us to identify the phosphatase SHP2 as a protein susceptible to sulfenylation under LSS. Given the dependence of FAK activity on SHP2 function, we explored the role of FAK under LSS conditions. FAK activation and subsequent endothelial NO synthase (eNOS) phosphorylation were promoted by LSS and both processes were dependent on NOX4, as demonstrated in lung endothelial cells isolated from NOX4-null mice. These results support the idea that LSS elicits redox-sensitive signal transduction responses involving NOX4-dependent generation of hydrogen peroxide, SHP2 sulfenylation, and ulterior FAK-mediated eNOS activation.

© 2015 Elsevier Inc. All rights reserved.

Vascular tone can be rapidly and tightly regulated by stress situations such as exercise or the need to immediately respond to superimposed threats. This fast reaction is primarily under the control of the central nervous system but also of local paracrine regulation within the cellular components of the vascular wall. Among the factors participating in the latter, nitric oxide (NO) is considered to be critical because of its importance in maintaining a vasodilatory basal tone and responding to changes in blood flow on both short- and long-term bases. Blood flow generates shear stress, which in itself is responsible for mechanotransducing effects resulting in specific biochemical and cellular signals. The shear stress exerted against the vessel wall, either laminar or turbulent, is determined by the type of flow. Laminar shear stress (LSS)[1] generally occurs in straight portions of the vessels and its magnitude is in the range of 12–14 dyn/cm^2[1]. LSS induces long-term gene expression changes leading to atheroprotection [2]. Nevertheless, acute increases in LSS also induce short-term membrane receptor-coupled protective responses, largely mediated by eNOS activation and NO synthesis, which cannot be explained by transcriptional regulation, as they require other prompt signaling mechanisms of activation such as phosphorylation. For example, LSS has been reported to activate the PECAM1-mediated cSrc signaling pathway by a series of successive phosphorylating

[1] *Abbreviations:* 2-OH-E$^+$, 2-hydroxyethidium; BAEC, bovine aortic endothelial cell; BSA, bovine serum albumin; cGMP, cyclic guanosine monophosphate; cSrc, proto-oncogene tyrosine protein kinase Src; DHE, dihydroethidine; EDHF, endothelial-derived hyperpolarizing factor; eNOS, endothelial nitric oxide synthase; E$^+$, ethidium; FBS, fetal bovine serum; FAK, focal adhesion kinase; GAPDH, glyceraldehyde-3-phosphate dehydrogenase; H_2DCFDA, H_2-dichlorofluorescein diacetate; LSS, laminar shear stress; IAM, iodoacetamide; MLEC, mouse lung endothelial cells; NEM, *N*-ethylmaleimide; NOX, NADPH oxidase; PECAM1, platelet endothelial cell adhesion molecule-1; PEG, polyethylene glycol; PFA, paraformaldehyde; PRX, peroxiredoxin; ROI, region of interest; ROS, reactive oxygen species; SHP2, SH2 domain-containing protein tyrosine phosphatase-2.

* Corresponding author.
E-mail address: slamas@cbm.csic.es (S. Lamas).

http://dx.doi.org/10.1016/j.freeradbiomed.2015.08.014
0891-5849/© 2015 Elsevier Inc. All rights reserved.

events [3]. In the past few years a growing interest has been placed on redox-dependent responses induced by LSS [4] and in this regard hydrogen peroxide (H_2O_2) has been reported as the biological messenger that mediates vasodilation in coronary arterioles after exposure to flow [5]. Hydrogen peroxide has been proposed as the hyperpolarizing factor in cGMP-independent vasorelaxation [6]. Several groups, including ours, have attempted to clarify the sources and mechanisms of generation of H_2O_2 in endothelial cells, as well as the downstream signaling induced by this molecule [4,7–9]. NADPH oxidases, whose unique known function is to produce ROS, are considered the major source of these ROS in the vasculature [10]. Although NOX1 and NOX2 isoforms were detected, we found that NOX4 was by far the most prevalent isoform in endothelial cells [8]. Several reports point toward a protective role of this enzyme. The absence of NOX4 in tamoxifen-inducible $NOX4^{-/-}$ mice attenuates angiogenesis in the femoral artery ligation model, an effect rescued by low concentrations of H_2O_2[11]. Furthermore, overexpression of NOX4 mediates protection by promoting EDHF-dependent vasodilatation, which is sufficient to lower blood pressure systemically [12]. Finally, we have reported that NOX4 favors NO production in endothelial cells exposed to LSS [8]. Hence, mounting evidence supports the concept that endogenous NOX4 protects the vasculature during ischemic or inflammatory stress [11].

One major mode of action of H_2O_2 is related to its capacity to interact with protein thiols and modify the cellular nucleophilic tone by promoting their cysteine oxidation. It can also induce the formation of sulfenic (–SOH), sulfinic ($–SO_2H$), and sulfonic acid ($–SO_3H$)-related moieties. Of these three, only the first is considered to play a physiological role [13,14]. Thiol oxidation to sulfenates occurs in redox-sensitive proteins bearing low-pK_a cysteines commonly located at catalytic or interaction domains, often resulting in altered signal transduction [15,16]. Because of its transient nature, its characterization is generally elusive, and only the recent incorporation of dimedone-based molecular tools has allowed the precise identification of specific sulfenate-modified cysteines [17,18]. With the aid of this methodology we now report the NOX4-dependent sulfenylation of the tyrosine phosphatase SHP2, which we believe is important for LSS-induced signaling responses leading to eNOS activation.

1. Materials and methods

1.1. Mouse models

Nox4-null mice ($NOX4^{-/-}$) were generated by targeted deletion of the translation initiation site and exons 1 and 2 of the gene (Genoway) [19]. DNA fragment constructs with exons 1 and 2 of the *Nox4* gene flanked by loxP sites and diphtheria toxin A and neomycin cassettes were electroporated into 129 sv embryonic stem cells, recombinant clones identified by PCR and Southern blot analysis, and injected into C57BL/6 blastocysts. $NOX4^{-/-}$animals were obtained by intercrossing the progeny and were backcrossed >10 generations into a C57BL/6 background. Eight-week-old $NOX4^{-/-}$ mice and age-matched wild-type mice were used in this study.

1.2. Study approval

The animals were housed and bred following all established regulatory standards, and all the experiments were performed in accordance with the guidelines of the European Parliament and of the European Council (Directive 2010/63/EU) "on the protection of animals used for scientific purposes," meeting the International Guiding Principles for Biomedical Research Involving Animals, and with the approval granted by the local ethics review board of the Centro de Biología Molecular "Severo Ochoa."

1.3. Cell culture

Bovine aortic endothelial cells (BAECs) were obtained from calf aortas at a local slaughterhouse and cultured as described [20]. In short, the aortas were subsequently washed with phosphate-buffered saline (PBS) and cells isolated by collagenase-mediated endothelial isolation. Cells were maintained in RPMI supplemented with 10% FBS and 0.1% penicillin/streptomycin. C57BL/6 wild-type and $NOX4^{-/-}$ mice (see above) were used to isolate mouse lung endothelial cells (MLECs). MLEC isolation was performed as previously described [8]. Experiments were done at semiconfluence between passages 2 and 7. Cells were starved overnight before the experiments.

1.4. Reagents

PEG–SOD (C4963) and PEG–CAT (catalase; s9549), iodoacetamide (IAM) (I1149), and *N*-ethylmaleimide (NEM) (E3876) were purchased from Sigma. H_2DCFDA (D-399) and dihydroethidium (DHE) (D-23107) came from Life Technologies, DCP-Bio1 (dimedone-B) (EE0021) was purchased from Kerafast, and PP2 (529573) was from Calbiochem.

1.5. Plasmid constructions, silencer molecules, and quantitative real-time PCR

Vector pHyPer-cyto (FP941) was purchased from Evrogen and pSypher-cyto from Addgene (48250). Custom small interfering RNA (siRNA) for NOX4 (5′-UCAUUCAAUCUAGAAAUUATT-3′–5′-UAAUUUCUAGAUUGAAUGATT-3′) was designed using the "Sfold" Web page (sfold.wadsworth.org). The best candidates were chosen on the basis of a total score for siRNA duplex higher than 15 and the sum of probabilities of unpaired target bases value higher than 13. Both siRNA molecules and their respective controls were obtained from Ambion. For all transfection experiments, BAECs at 60% of confluence were transfected with Lipofectamine 2000 (Invitrogen, Carlsbad, CA, USA) for 6 h and left to overexpress or silence the corresponding protein for 48 h after the transfection. RNA was isolated using TRIzol reagent (Invitrogen). cDNA synthesis was undertaken using an iScript cDNA synthesis kit (170–8891, Bio-Rad). Quantitative real-time PCR was performed using a C1000 Thermal Cycler CFX96 (Bio-Rad). The endogenous NOX4 cDNA was amplified by SYBR Green Supermix (172–5201, Bio-Rad) using the following primers: forward primer 5′-ACTTTTCATTGGGCGTCCTC-3′; reverse primer 5′-TGCTGTGGACCCAGTTCT-3′. GAPDH was used as the housekeeping gene.

1.6. Laminar shear stress induction

Laminar shear stress at 12 dyn/cm^2 was generated by using a "cone and plate" system as previously described [8,21]. In immunofluorescence experiments shear stress was generated by the Ibidi pump system (Ibidi, Martinsried, Germany). Six-channel μSlide$^{0.4}$ multiwells were coated with 0.2% gelatin in PBS and 30 μl of 9×10^5 cells/ml were seeded into each channel. After treatments with probes, the cells were exposed to LSS with the cone and plate or Ibidi system at 37 °C for the indicated times.

1.7. HPLC-based detection of superoxide

Detection of superoxide anion was carried out as previously described [22]. Semiconfluent BAECs cultured in 60- mm-diameter culture dishes were pretreated with 10 μM DHE for 2 h and

exposed to LSS. Cells were harvested in 120 µl PBS, 0.1% Triton X-100, and frozen at −80 °C overnight. One hundred microliters of lysate was mixed with 250 µl of 100% butanol, vortexed for 1 min, and centrifuged for 1 min at maximum speed, and the alcoholic phase was recovered and dried. The extracted component was resuspended in 50 µl of HPLC-grade water and injected into the HPLC system (Alliance Separation Module 2695, Waters) into a Mediterranea Sea_{18} HPLC column (Teknokroma, C18, 250 × 4.5). To detect the two subproducts, 2-hydroxyethidium (2-OH-E^+) and ethidium (E^+), elution was monitored at 490 nm of excitation and 567 nm of emission wavelength (Multi λ Fluorescence Detector 2475, Waters). A continuous gradient was applied to the column and preequilibrated with buffer A (10% CH_3CN/0.1% trifluoroacetic acid (TFA)), and the elution was performed with continuous gradient from 80% buffer A/20% buffer B (99.9% CH_3CN/0.1% TFA) to 100% buffer B. The area under the peak detected for 2-OH-E^+ (superoxide) was normalized by the protein concentration of each sample (BCA, Pierce).

1.8. Cell oxidant state determination and H_2O_2 detection in endothelial cells

To measure hydrogen peroxide formation semiconfluent BAECs were starved overnight in RPMI without phenol red and pretreated or not with 20 units of PEG–CAT for 1 h where indicated. Thirty minutes before the appropriate treatments, 10 µM H_2DCFDA was loaded onto the cells. BAECs were exposed to LSS for various periods or treated with 100 µM H_2O_2 for 30 min as a positive control. The cells were washed twice with ice-cold PBS and trypsinized and the fluorescence of 15,000 cells was analyzed in a BD FACSCalibur (Becton–Dickinson) cytometer at 530 nm. To specifically measure H_2O_2, 80% confluent BAECs seeded in a 0.2% gelatin-precoated Ibidi µSlide$^{0.4}$ multiwell plate were transfected with pHyPer-cyto and pSypHer-cyto vectors. After 48 h of transfection, the cells were preincubated with PEG–CAT for 1 h where indicated. Cells were exposed to 12 dyn/cm^2 LSS with the Ibidi perfusion system for 15 min or H_2O_2 as positive control using a temperature-controlled station coupled to an AF 6000 LX Leica microscope and HCX PL APO 40 × /1.25–0.75 Oil CS objective. Cell fluorescence was detected at 405 nm excitation and 520 nm emission and 494 nm excitation and 520 nm emission consecutively every 30 s for 15 min [23]. The quantification was carried out with Fiji software. One region of interest (ROI) to the cell (specific signal) and two ROIs surrounding the cell (background) were defined for each cell and channel. The mean fluorescence intensity of the two background ROIs was subtracted from the fluorescence intensity of the ROI signaling of each cell and time point, and the ratio between the signals obtained at 490 and 405 nm was calculated. To present the fluorescent signal in the video images, the "16_color" look-up table was applied to the final ratio signal.

1.9. In vitro and ex vivo immunofluorescence

The buffers used in in vitro immunofluorescence were deoxygenated as described below under *Sulfenylated protein analysis*. Six-channel µSlide IV$^{0.4}$ multiwells were coated with 0.2% gelatin in PBS and 30 µl of 10^6 cells/ml was seeded into each channel. Semiconfluent BAECs were starved overnight before LSS exposure. The cells were preincubated with 20 units of PEG–CAT where indicated and loaded with 50 µM dimedone-B. The cells were exposed to 12 dyn/cm^2 LSS with the Ibidi perfusion system for 15 min or treated with H_2O_2 as positive control in a temperature-controlled station. After exposure to LSS and to the indicated treatments, the cells were washed with ice-cold PBS, fixed for 15 min with 2% cold paraformaldehyde (PFA), and permeabilized for another 15 min with 0.25% Triton X-100 in PBS, 100 mM IAM, and 100 mM NEM. The cells were blocked with 3% BSA in PBS and incubated with 1:200 anti-SHP2 primary antibody solution at 4 °C overnight. Then the cells were incubated for 1 h at room temperature with 1:200 anti-mouse-555 and streptavidin-488 solutions. Fluorescence was detected with a Zeiss LSM 510 Meta confocal microscope. Images were analyzed with Fiji software. The colocalization study of dimedone-B and SHP2 protein was carried out with the Colocalization Highlighter Fiji plug-in. For ex vivo aortic detection of sulfenylated cysteines, 8-week-old NOX4$^{-/-}$ mice were anesthetized and perfused with 10 ml of sterile saline solution, and their aortas were excised and fixed in 4% PFA for 4 h. Using a stereomicroscope Leica MZ6, the fat and adventitia layers were cleaned, the intercostal arteries were eliminated, and the aorta was cut along the vessel. Vessels were permeabilized with 0.1% Triton X-100 for 4 h at 4 °C, blocked with donkey serum, and incubated with 50 µM dimedone-B in 3% BSA in PBS for 2 h at room temperature and with anti-PECAM-1 antibody solution overnight at 4 °C. Aortas were mounted "en face" in coverslides and fluorescence was detected with a Zeiss LSM 510 multiphoton confocal microscope. For the quantification, the projection of all confocal images of a field was obtained and the mean fluorescence of 20 ROIs per projection was analyzed. This approach was carried out for three images per aorta in aortas from nine wild-type or NOX4$^{-/-}$ mice.

1.10. Western blot analysis

Endothelial cells were cultured to subconfluence, starved overnight, and pretreated with 5 µM PP2 for 1 h as indicated and exposed to LSS 12 dyn/cm^2 for 15 min. Cells were washed with PBS and harvested in "CHEES" lysis buffer (20 mM Hepes, 150 mM NaCl, EDTA 5 mM, EGTA 5 mM, 2% SDS, 0.5% NP-40, 0.5% Triton X-100, 0.5% sodium deoxycholate, 20 mM NaF, 20 mM Na_2PO_4, 200 mM sodium orthovanadate). Homogenates were centrifuged at 12,000 rpm for 15 min at 4 °C and the protein concentration was estimated by the BCA method (Thermo Scientific). Forty micrograms of protein samples was analyzed by SDS–PAGE and immunoblotted against anti-FAK (Sigma), anti-pFAK (Cell Signaling), anti-eNOS (BD Transduction Laboratories), anti-peNOS (1177) (Cell Signaling), anti-PRXs–SO_3 (AB Frontier), anti-GAPDH–SO_3 (AB Frontier), anti-SHP2 (BD Transduction Laboratories), or anti-NOX4 [24]. Protein signals were quantified by densitometry using Scion Image software and statistically analyzed with GraphPad Prism 5.0 software.

1.11. Sulfenylated protein analysis

Protein sulfenic form detection by SDS–PAGE was carried out as described previously [17]. All buffers used for dimedone-B adduct detection were prepared with boiled water and maintained in negative pressure to be deoxygenated before being used. Deoxygenated dimedone-B lysis buffer (Tris, sodium deoxycholate, NP-40, Triton X-100, protease inhibitor cocktail, NaF, Na_2PO_4, 200 mM sodium orthovanadate, 100 mM NEM, 100 mM IAM) was prepared just before use. Subconfluent endothelial cells starved overnight were pretreated with 50 µM dimedone-B with or without PEG–CAT for 1 h. Then the cells were exposed to 12 dyn/cm^2 LSS for 15 min or 300 µM H_2O_2 for 30 min, extensively washed with 1 × PBS and harvested in deoxygenated dimedone-B lysis buffer, and centrifuged at 12,000 rpm for 15 min at 4 °C, and protein concentration was quantified by BCA assay. To test general proteome sulfenylation, 40 µg of protein from homogenates was analyzed by SDS–PAGE, transferred onto nitrocellulose membranes, blocked with 3% nonfat milk in TBS–Tween, and incubated with infrared-labeled streptavidin (LI-COR system). Protein signals

were quantified by Scion Image and statistically analyzed with GraphPad Prism 5.0 software.

For sulfenylated protein pull-down purification, 200 μg of protein homogenates was incubated overnight at 4 °C with 50 ml of neutravidin beads (Thermo, Pierce), previously equilibrated with deoxygenated PBS. After the incubation, the unbound fraction was discarded and beads were washed extensively with deoxygenated PBS and eluted in sample buffer (without reductants) and boiled for 10 min at 95 °C. Eluted fractions were analyzed by SDS–PAGE and Western blot against infrared-labeled streptavidin and anti-SHP2.

For proteomic analysis, pull-down fractions were loaded onto a polyacrylamide gel and concentrated at the stacking–running interphase, excised, and processed as previously reported [25,26].

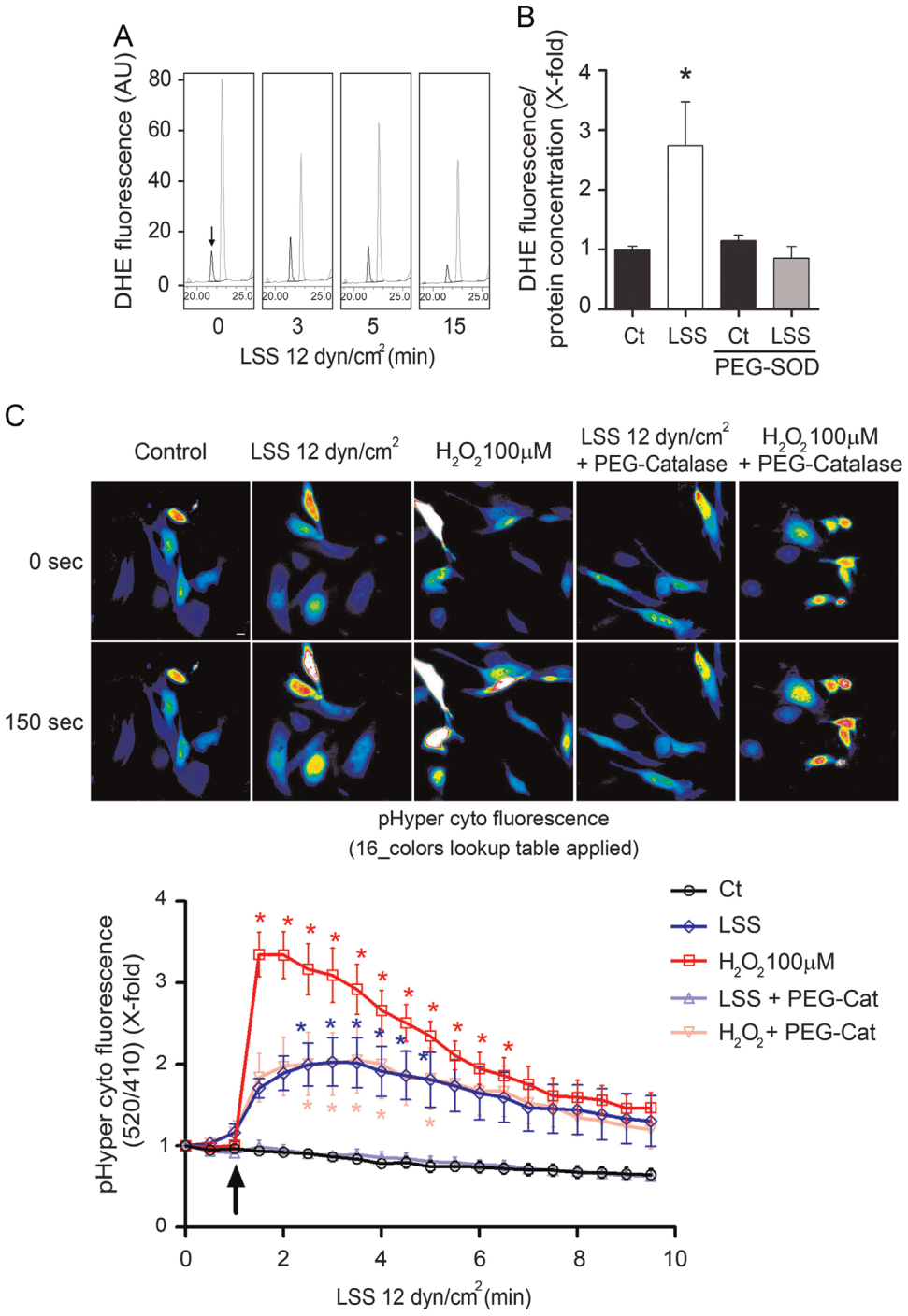

Fig. 1. Early detection of superoxide radical anion and H_2O_2 in endothelial cells exposed to LSS. (A) BAECs were preincubated with 10 μM DHE, exposed to LSS, and analyzed by HPLC. Representative sections of chromatograms for 0, 3, 5, and 15 min of exposure with OH-ethidium (black) and ethidium (gray) peaks are shown. The peak corresponding to superoxide radical is marked with a black arrow. (B) BAECs were preincubated with DHE or DHE and PEG–SOD and exposed to LSS for 3 min and the fluorescence analyzed by HPLC. Bar graph represents superoxide radical detection after correction by protein concentration and normalization ($n=3$). (C) BAECs were transiently transfected with 2 μg of pHyper-Cyto vector for 48 h, starved overnight, and exposed to LSS and 100 μM H_2O_2, with or without PEG–CAT. (Top) Images represent cells exhibiting fluorescent signals after detection as stated under Materials and methods after 16_colors lookup table from Fiji software transformation to allow representation of changes in the fluorescence intensity. (Bottom) Ratiometric measurements were calculated for each time point and cell. The black arrow indicates the time when reagents were added ($n=4$). Scale bar indicates 10 μm. $^*p < 0.05$ vs control. Bar graphs represent the mean ± SEM for the indicated *n*.

Bands were dehydrated with 100% acetonitrile, reduced with 10 mM dithiothreitol, alkylated with 54 mM IAM, and trypsinized. The peptide mixture was extracted from the gel with 12 mM ammonium bicarbonate, pH 8.8, and desalted with OMIX C18 tips (Agilent). Samples were analyzed by LC–MS/MS with an Orbitrap Elite Hybrid Ion Trap–Orbitrap mass spectrometer (Thermo Scientific). Peptides were identified from the MS/MS spectra using Sequest running under Proteome Discoverer 1.4 as described [27,28].

1.12. Statistics

All data are presented as the mean ± SEM. One-way ANOVA was used when data adjusted to normality and homoscedasticity, followed by post hoc Tukey's test. When data did not adjust to a normal distribution or the variances were different, nonparametric tests were used to compare two conditions. A $p < 0.05$ was considered significant.

2. Results

2.1. Short-term exposures to LSS induce the generation of superoxide radical anion and hydrogen peroxide in endothelial cells

We have previously described that LSS is able to generate hydrogen peroxide within signaling range levels [8]. Whereas the formation of superoxide radical anion was detected, the temporal course linking its formation to that of hydrogen peroxide had not been characterized in detail. To clarify this issue, the generation of superoxide was specifically analyzed using HPLC-based fluorescence detection of DHE products [29] including positive and negative controls for superoxide generation as described previously [30,31]. A typical HPLC chromatogram shows the two peaks generated by the transformation of DHE to 2-OH-E^+ and E^+, the first one considered specific for superoxide generation (Supplementary Fig. 1). The increase in 2-OH-E^+ production in response to cyclosporin was abolished when cells were pretreated with Tiron, a superoxide scavenger. Other superoxide generators such as DMNQ also increased 2-OH-E^+ in a concentration-dependent fashion (Supplementary Fig. 1A). In our model we observed a maximum superoxide generation at 3 min of LSS exposure (Supplementary Figs. 1B, 1C, and 1D and Fig. 1A) that decreases after 15 min. This signal was abolished by PEG–SOD pretreatment (Fig. 1B). We conclude that LSS induces superoxide production at very early time points, as detectable by a very specific method. A wide range of LSS exposure times showed that endothelial cells generated a biphasic wave of superoxide (Supplementary Fig. 1D), with an initial burst after 3 min and a second production peak at 1 h of LSS exposure, consistent with our previous reported observations [8].

Because hydrogen peroxide, in contrast to the superoxide radical anion, fulfills all the key requisites for being considered a signaling molecule [32], we evaluated the cellular oxidant state index by using H_2DCFDA under the same conditions of LSS where we had detected increased levels of superoxide radical anion. We observed an expected moderate but significant increase in fluorescence after 5 min of LSS (Supplementary Fig. 2A), an observation compatible with the potential dismutation of superoxide radical anion into hydrogen peroxide as a contributing species to the increase in the aforementioned index. PEG–CAT pretreatment prevented the increase in H_2DCFDA-associated fluorescence, suggesting the participation of H_2O_2 in this response (Supplementary Figs. 2A–2D). However, the fact that the specificity of H_2DCFDA is highly controversial [33,34] prompted us to use a more sensitive and specific tool such as the pHyper-cyto (pHyper) vector [23]. In endothelial cells transfected with pHyper we detected a clear increase in the fluorescent signal 30s after exposure to LSS (Fig. 1C; Supplementary Time-Lapse Movies 1 and 2). As expected the response observed was lower than that induced by H_2O_2 cell treatment (Fig. 1C; Supplementary Time-Lapse Movie 3), supporting the signaling role of H_2O_2 promoted by LSS. Pretreatment with PEG–CAT prevented and reduced the increase in the signal induced by LSS and H_2O_2, respectively (Supplementary Time-Lapse Movies 4 and 5). The fluorescence associated with pHyper reached its peak between 1.5 and 2.5 min after the initiation of LSS, time points at which superoxide presence had already been detected. Given the fact that pHyper fluorescence may be sensitive to pH variations [23,35] and the intracellular acidification induced by LSS [36], we tested the fluorescence changes in the specifically pH-sensitive pHyper C199S mutant, pSypHer-cyto, to exclude that pH changes were accounting for the increased fluorescent signals. Endothelial cells transfected with the pSypHer-cyto vector exposed to LSS showed a slight increase in fluorescence compared with BAECs transfected with pHyper-cyto under the same conditions (Supplementary Fig. 2E), indicating that the fluorescence detected with pHyper reflects H_2O_2 generation in response to LSS. This close temporal correlation between superoxide and hydrogen peroxide formation suggests that this method is probably more suited to reflecting acute changes in the levels of these ROS. The fading of the H_2O_2-derived signal is probably related to the transient nature of the pHyper-related fluorescence, rather than to a decrease in the abundance of H_2O_2, as data obtained with H_2DCFDA suggest (Supplementary Fig. 2A). We take these results to indicate that LSS generates superoxide radical anion in endothelial cells, which is rapidly converted into H_2O_2 at very early time points.

Supplementary material related to this article can be found online at http://dx.doi.org/10.1016/j.freeradbiomed.2015.08.014.

2.2. LSS-mediated H_2O_2 generation increases the sulfenylation of the endothelial proteome

To detect the presence of sulfenylated thiols in endothelial cells exposed to LSS, cells were pretreated with dimedone-B and then exposed to LSS or H_2O_2. In time-course experiments we observed a significant increase in the dimedone-related streptavidin signal at 15 min of LSS exposure (Supplementary Fig. 3). Exposure to LSS and treatments with H_2O_2 induced consistent changes in general proteome sulfenylation (Fig. 2A and B). Interestingly, pretreatment of cells with PEG–CAT prevented the sulfenylation of proteins, supporting the role of H_2O_2 as the oxidizing species. Of notice, only exogenous treatments with H_2O_2 promoted overoxidation of the well-known redox sensors PRXs and GAPDH, whereas PEG–CAT prevented this effect (Fig. 2A, bottom, and Supplementary Fig. 3). In contrast, LSS induces the increase in hydrogen peroxide and subsequent reversible protein sulfenylation at signaling range concentrations, which appear to be unable to induce overoxidation of PRXs. Nevertheless, the absence of proven linearity of biotinylation as a means to accurately reflect sulfenylation at high concentrations of hydrogen peroxide poses a word of caution on the establishment of close parallelisms between both approaches. This effect on sulfenylation was also corroborated by cell immunofluorescence, confirming the membrane permeability of the probe. Endothelial cells exposed to LSS or treated with H_2O_2 exhibited higher fluorescence intensity than control cells, and PEG–CAT pretreatments significantly abrogated this increase (Fig. 2C). These results confirm that LSS generates signaling levels of H_2O_2 that result in detectable sulfenylation of endothelial proteins.

2.3. NOX4 mediates H_2O_2 generation in LSS

We have previously reported that NOX4 is the most abundant NOX isoform in endothelial cells and that it plays a critical role in LSS-induced responses [8]. Given the dual capacity of NOX4 to

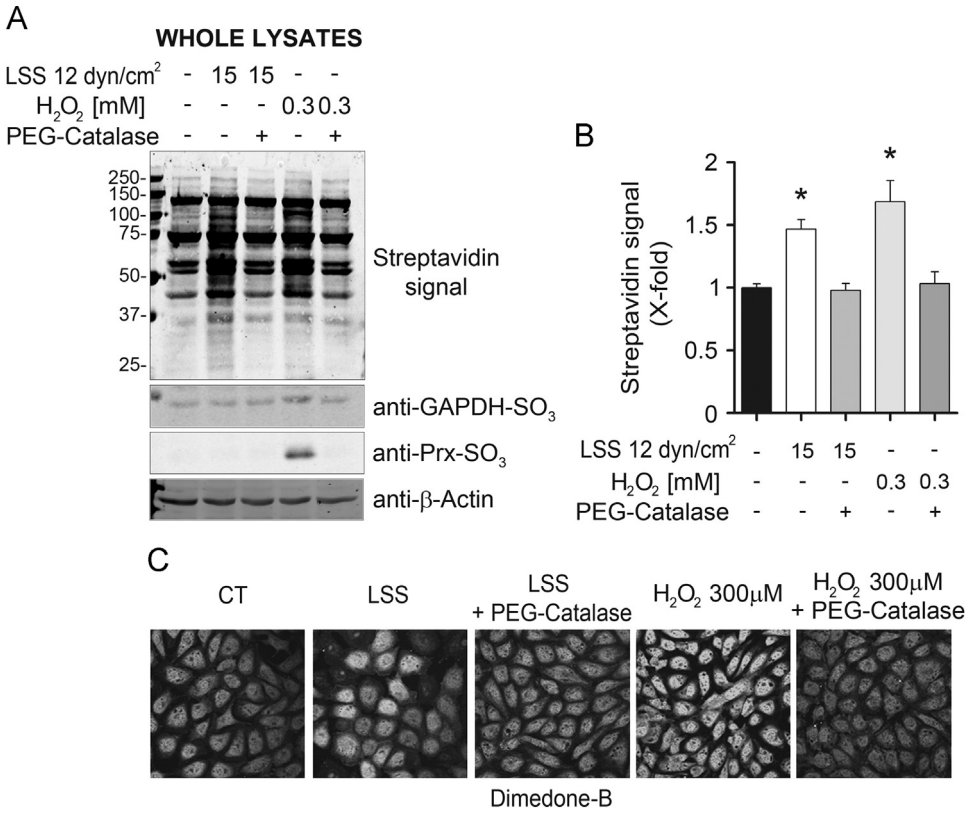

Fig. 2. LSS-induced H_2O_2 increases global sulfenylation of the endothelial proteome. (A) BAECs were preincubated or not with PEG–CAT, exposed to dimedone-B for 1 h, and treated with H_2O_2 or LSS. General proteome sulfenylation and GAPDH and PRX overoxidation were analyzed by Western blot. (B) Bar graph represents the mean ± SEM of the densitometric quantification of bands corresponding to sulfenylated proteins and normalized to control samples ($n=4$). $^*p < 0.05$ vs control. (C) Endothelial cells were seeded onto six-channel μSlide IV$^{0.4}$ multiwells, pretreated with or without PEG–CAT, incubated with dimedone-B for 1 h, and treated with H_2O_2 or exposed to LSS in the Ibidi flow generator for 15 min. Representative fluorescence images for sulfenylated proteins are shown.

generate both superoxide radical anion and hydrogen peroxide [29,37] we evaluated its role in superoxide production after knocking down NOX4 in endothelial cells (Supplementary Figs. 4A and 4B). In HPLC-based superoxide detection experiments we observed that silencing of NOX4 in endothelial cells decreased superoxide production after 3 min of LSS (Fig. 3A). The cellular oxidant state index as reflected by H_2DCFDA fluorescence in LSS-treated endothelial cells was also reduced to control levels under this condition (Fig. 3B). This indicates that endothelial cells produce ROS in a NOX4-dependent manner in response to LSS. Hence we tested if protein sulfenylation could also be regulated by NOX4. NOX4 abrogation was associated with a significant decrease in LSS-dependent endothelial protein sulfenylation (Fig. 3C).These results indicate that NOX4 is crucial for peroxide-dependent early protein sulfenylation in endothelial cells exposed to LSS.

2.4. The tyrosine phosphatase SHP2 is sulfenylated by LSS-induced H_2O_2 production

Phosphatases are among the proteins that are well known to become modified by sulfenylation [38–41] and as a consequence of this modification they regulate several signal transduction pathways [42]. To gain insight into the nature of specific redox-sensitive sulfenylated phosphatases in endothelial cells subjected to LSS we employed mass spectrometry. The tryptic peptides obtained from purified fractions of sulfenylated protein were analyzed by ESI–LC–MS/MS and scanned for bovine proteins. We identified 449 proteins in the extracts; some of them were present in LSS and/or H_2O_2-treated samples but not in control ones (Supplementary Table 1). SHP2 (PTPN11) was identified among the subset of modified proteins that were detected only after LSS or H_2O_2 treatments (Fig. 4A). The sulfenic oxidation of SHP2 under these conditions was confirmed by Western blot of the purified fractions, which demonstrated an increase in the streptavidin-associated signal of endothelial cells exposed to LSS or treated with H_2O_2 (Fig. 4B). This effect was prevented by pretreating cells with PEG–CAT, attesting to the role of LSS-generated H_2O_2 in SHP2 sulfenylation. Confocal microscope experiments revealed an increased signal in biotinylated dimedone-B and SHP2 in LSS and H_2O_2-treated endothelial cells with apparent de novo plasma membrane colocalization indicated with red arrows, more visible with LSS and H_2O_2 (Fig. 4C). The role of NOX4 in LSS-mediated sulfenylation of SHP2 was confirmed by the abrogation of the biotinylated SHP2 signal increase in NOX4-silenced endothelial cells subjected to LSS (Fig. 4D). We take these data to indicate that NOX4-mediated H_2O_2 generation is necessary for SHP2 sulfenylation and promotes its occurrence with a topology compatible with plasma membrane localization.

2.5. NOX4 modulates the upstream signaling cascade of LSS-induced eNOS activation

SHP2 has been reported to regulate FAK activation in breast tumor epithelial cells, inducing cell migration and lamellipodia formation [43]. Furthermore, direct interaction between SHP2 and FAK contributing to the regulation of its phosphorylation state has been described, reporting that a SHP2-negative dominant mutant was unable to reproduce FAK dephosphorylation induced under ephrin stimulation [44]. FAK has been shown to regulate NO-mediated flow-induced vasodilation, and direct inhibition of FAK was able to blunt this response [45]. In this study we demonstrated that FAK inhibition abrogated FAK phosphorylation and

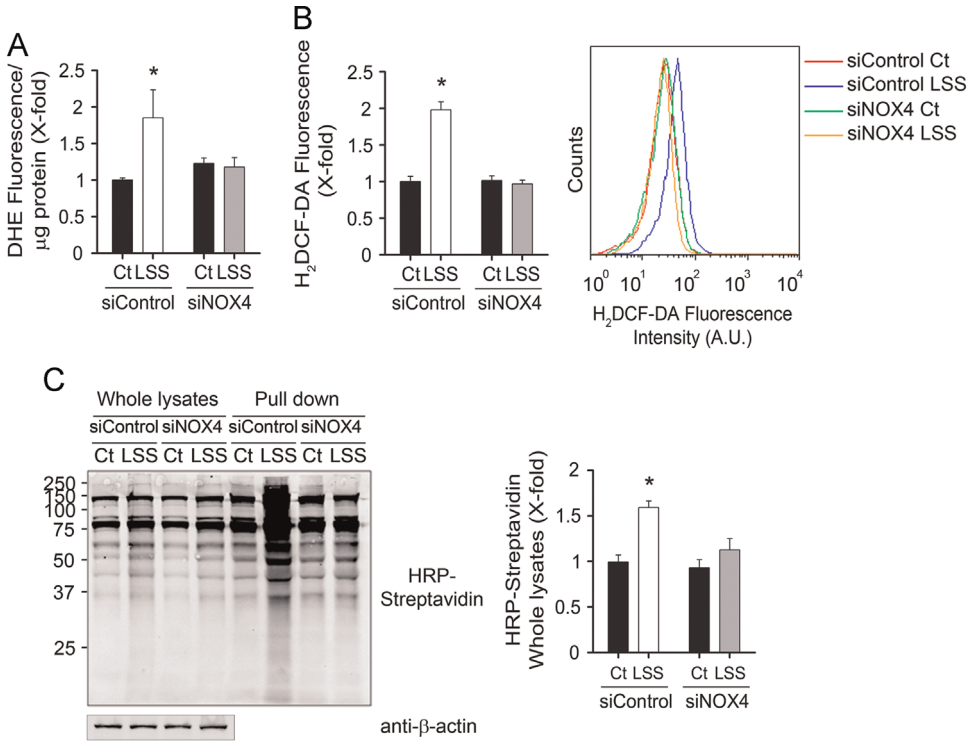

Fig. 3. Role of NOX4 in ROS production and proteome sulfenylation. Endothelial cells were transfected with NOX4 siRNA (siNOX4) or control siRNA (siControl) for 48 h and then starved overnight. (A) BAECs were preincubated with DHE and exposed to 3 min of LSS and superoxide production was determined by HPLC. Bar graph depict the mean ± SEM of DHE fluorescence ($n=5$), $^*p<0.05$ vs control. (B) Cells were preincubated with H_2DCFDA and exposed for 5 min to LSS and cell fluorescence was analyzed by flow cytometry. Bar graph depicts the mean ± SEM of H_2DCFDA fluorescence ($n=3$), $^*p<0.05$ vs control. A representative experiment is shown on the right. (C) Cells were preincubated with dimedone-B and exposed to 15 min of LSS. Sulfenylated proteins were purified from total protein homogenates by avidin-based pull-down assay, and samples and purified fractions were analyzed by SDS–PAGE. Lower blot under whole lysates depicts β-actin as the corresponding loading control. Shown on the left is a representative blot from $n=3$. The bar graph on the right depicts the mean ± SEM of the densitometric analysis of the HRP–streptavidin signal from the whole-protein lysates ($n=3$), $^*p<0.05$ vs control.

concomitantly eNOS activation (Fig. 5A). To confirm that this effect was dependent on NOX4, MLECs obtained from wild-type and NOX4$^{-/-}$ mice were exposed to LSS. Endothelial cells from NOX4$^{-/-}$ animals failed to exhibit pFAK and peNOS increased levels after short-term exposures to LSS (Fig. 5B), suggesting that NOX4-mediated ROS production is necessary and sufficient to promote LSS-mediated eNOS activation. This provides direct evidence for the role of NOX4 as an upstream key player in the signaling cascade of LSS-dependent eNOS activation and indirectly indicates a potential role for SHP2 sulfenylation. We next evaluated if NOX4 could be modulating protein sulfenylation in vascular tissue by en face dimedone-B endothelial staining. Protein sulfenylation was clearly higher in endothelial layers from WT mice than in those from NOX4$^{-/-}$ mice (Fig. 5C and Supplementary Fig. 5). The location of the dimedone-B signal was coincident with the PECAM1 signal, suggesting that the dimedone-B signal is circumscribed to the endothelial layer as the muscle layer did not exhibit signals of either dimedone-B or PECAM1. It is noteworthy that the levels of eNOS phosphorylation were significantly reduced in arteries from NOX4$^{-/-}$ mice, thus supporting a close correlation between NOX4 presence and eNOS activation (Fig. 5D). Overall, we take these data to support the importance of NOX4-mediated protein sulfenylation, including that of SHP2, in eNOS activation under LSS conditions.

3. Discussion

The regulation of vascular tone is a complex process involving both long- and short-term mechanisms and responses. Blood flow elicits both types of temporal homeostatic adaptations as a result of its ability to trigger immediate receptor-coupled signaling cascades and to promote specific transcriptional programs. Well-known examples are the ability of shear stress to induce p38-MAPK activation after 1 h in a ROS-dependent manner [8] or the capacity of epidermal growth factor (EGF) to induce short-term phosphorylation and activation of PRX proteins in rat smooth muscle cells [16]. It is accepted that LSS is generally atheroprotective [2,46], whereas turbulent or oscillatory SS induces the expression of proinflammatory mediators, which favor atherogenesis [47]. We have previously described the importance of redox-mediated early responses to LSS [7,8], but we now report that a very relevant part of LSS-induced redox responses in the endothelium is germane to the capacity of NOX4 to promote the specific reversible oxidation of proteins. Furthermore we provide evidence for LSS-associated sulfenylation of SHP2 and we propose that LSS-mediated generation of peroxide ultimately results in FAK phosphorylation and eNOS activation in blood vessels.

One major challenge in the field of redox signaling and cardiovascular responses is the difficulty in characterizing the nature of the ROS involved and in specifically demonstrating their physiological role by identifying appropriate targets within signaling pathways. We have approached the first problem by using available methods that may unambiguously define which kind of ROS is being generated. In this regard, the use of HPLC-based superoxide radical determination and HyPer-based peroxide fluorescence detection allowed us to establish a temporal response pattern to LSS by which superoxide generation takes place at very early stages and precedes by a short interval the formation of hydrogen peroxide. This is consistent with a model whereby dismutation of superoxide would account for the majority of peroxide production [37]. Importantly, from a physiological standpoint,

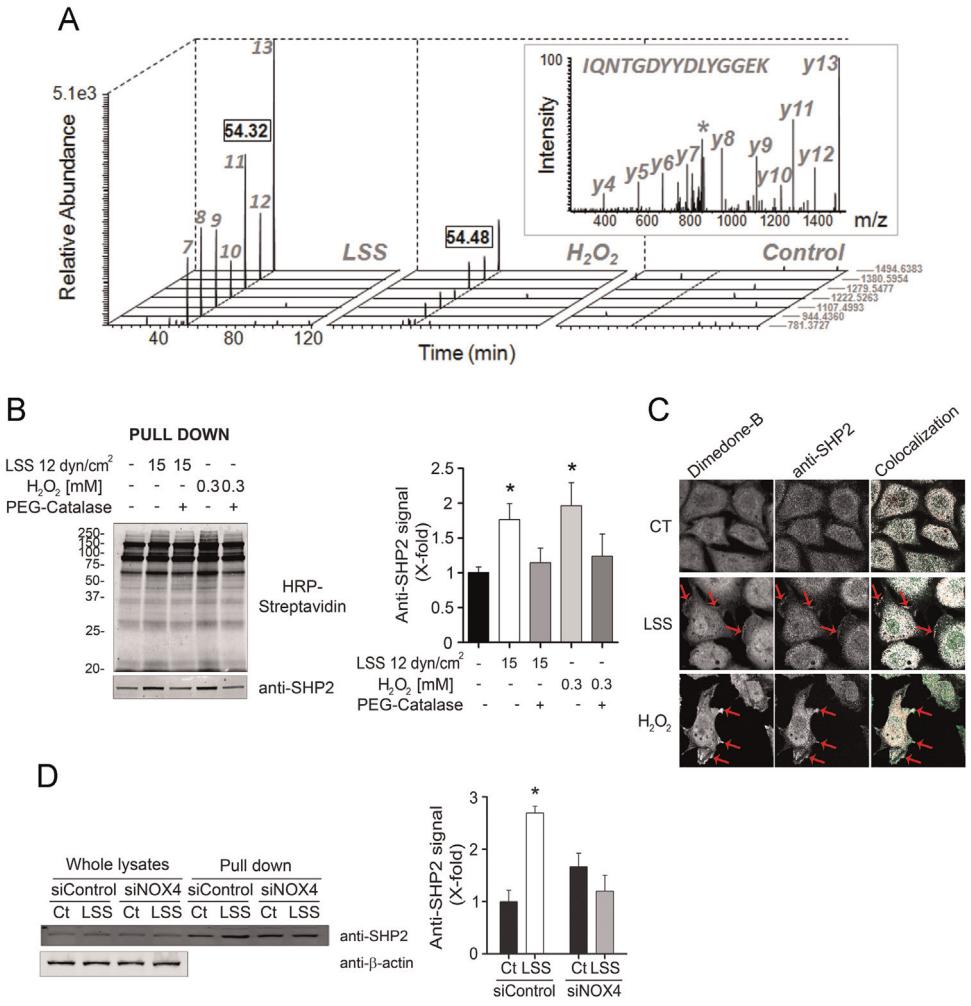

Fig. 4. LSS induces NOX4-dependent SHP2 sulfenylation. (A) Extracted ion-chromatogram traces of selected fragments from the peptide IQNTGDYYDLYGGEK belonging to SHP2 in the samples containing sulfenylated proteins after LSS or H_2O_2 treatment or without treatment (control). Fragments from the y-series are labeled over the corresponding peak. Inset: MS/MS spectrum from the peptide at 54.32 min in the LSS-treated sample. (B) The blot (left) shows the streptavidin signals after pull down from protein samples of endothelial cells pretreated with dimedone-B, with or without PEG–CAT, and treated with H_2O_2 or exposed to LSS. The lower blot corresponds to a representative immunoblot for SHP2 and the bar graph shows the densitometric quantification of the signal from three independent experiments (mean ± SEM, $n=3$). (C) Endothelial cells were pretreated with dimedone-B for 1 h and then treated with H_2O_2 or exposed to LSS in the Ibidi flow generator for 15 min. Representative fluorescence images for sulfenylated proteins and SHP2 are shown. The colocalization of cysteine sulfenylation and SHP2 is shown on the right highlighted in white pixels and indicated with red arrows, using the highlighter Fiji plug-in. (D) After siRNA treatments (control or NOX4) for 48 h, BAECs were preincubated with dimedone-B and exposed to 15 min of LSS. Sulfenylated proteins were purified from total lysates by avidin-based pull-down assay and analyzed by SDS–PAGE and immunoblotted for SHP2 (left). Lower blot under whole lysates depicts β-actin as the corresponding loading control. The bar graph (right) represents densitometric quantifications from three independent experiments (mean ± SEM) normalized to whole-lysate control samples, $^*p < 0.05$ vs control.

hydrogen peroxide, rather than the superoxide radical anion, fulfills all the necessary criteria to be considered a second messenger [32], and a significant amount of evidence attests to its vasodilatory role in the vascular wall [6,8,48–50]. In this work, the decrement in ROS production induced by a permeative peroxide scavenger such as PEG–CAT clearly points to the production of H_2O_2 after LSS exposure. Moreover, the results obtained in cells with the pHyper vector and its correspondent pH sensor control, pSypHer, together with correlative changes in the presence of reduced or suppressed levels of NOX4 are definitely compatible with the role of peroxide as a physiological activator of vasodilation. We were able to identify a member of the protein tyrosine phosphatase (PTP) family as a target for NOX4-dependent peroxide-mediated sulfenylation under conditions of LSS. MS studies allowed us to spot SHP2 among the proteins specifically sulfenylated after treatment with LSS, which in contrast was unable to overoxidize exquisite peroxide sensors such as PRXs or GAPDH. This result is consistent with the generation of peroxide within signaling levels, rather than within toxic or pharmacological concentrations. Included in the group of redox-sensitive proteins, PTPs represent key players in signal regulation. PTPs bear a specific signature motif, $HC(X)_5R(S/T)$, which provides a unique environment for the catalytic Cys residue to achieve a low pK_a favored by the conserved Arg residue [51]. Hence the Cys residue behaves as a good nucleophile at neutral pH but also is highly susceptible to oxidation [52]. Even though the structure–function relationships of redox-sensitive thiols present in PTPs have been the object of extensive study [53,54], current consensus in the field supports that reaction of phosphatases with peroxide are not kinetically favored compared to professional redox sensors such as PRXs or endogenous intracellular antioxidants present at high concentrations, such as glutathione [55]. Nevertheless, recent evidence allows one to reconcile views combining an immediate reaction between peroxide and PRXs, while still allowing ulterior oxidative modifications of redox-sensitive proteins mediated by second-order reactions [16]. Hence, it would be eventually possible that SHP2 suffers reversible sulfenylation after exposure to low concentrations of peroxide, even in the presence of PRXs and

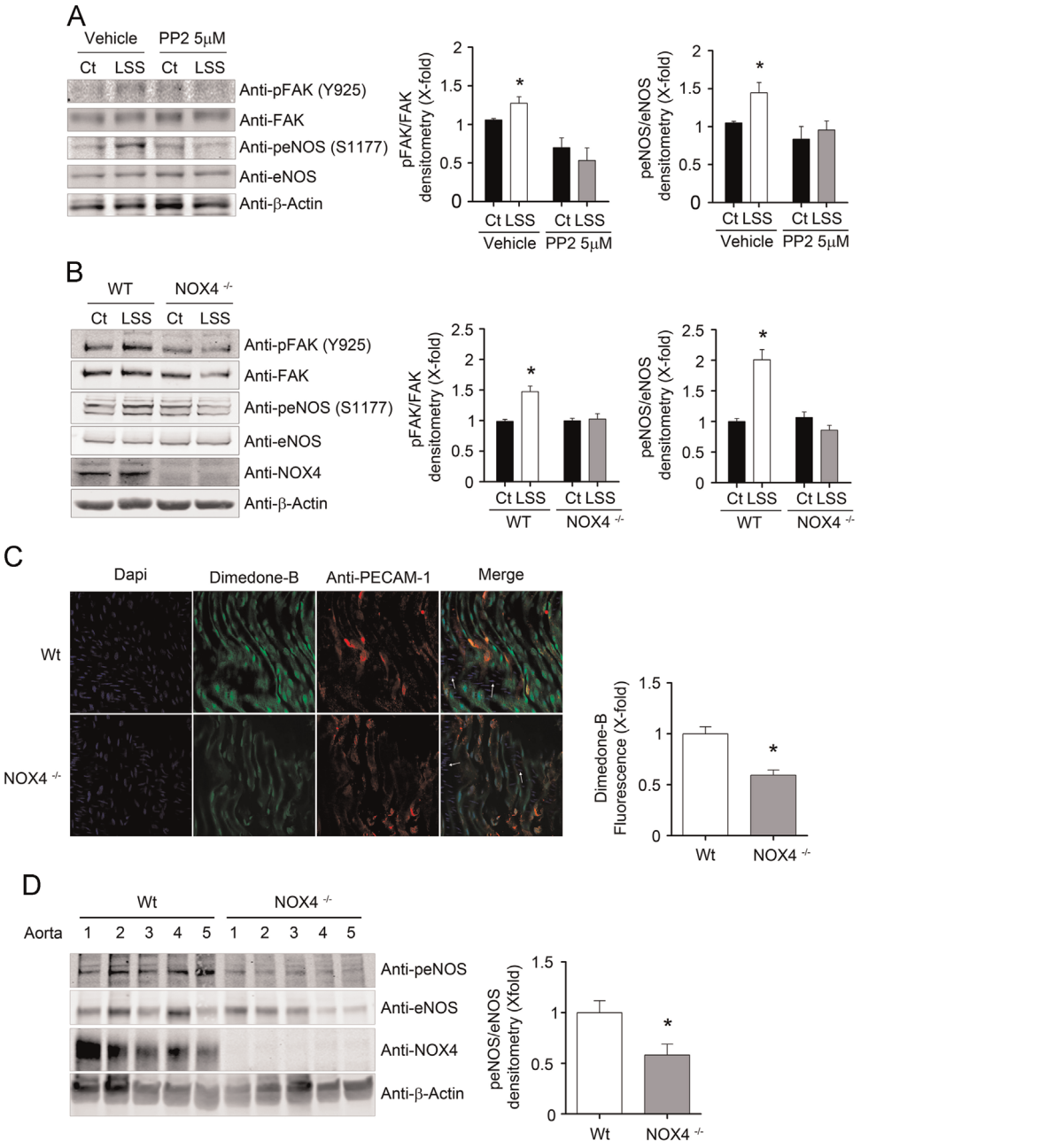

Fig. 5. NOX4 role in LSS-induced signaling and ex vivo oxidation. (A) After overnight serum deprivation, BAECs were pretreated or not with the FAK chemical inhibitor PP2 for 1 h and exposed to LSS for 15 min. Shown on the left is a representative immunoblot for FAK and eNOS using phospho-specific or total protein antibodies. Bar graphs on the right depict densitometric quantifications of pFAK and peNOS protein levels, mean ± SEM, $n=3$, after respective corrections by total protein and normalized to control conditions (Ct, vehicle in the absence of LSS), $^{*}p<0.05$ vs control. (B) After overnight serum deprivation, MLECs isolated from either wild-type (WT) or NOX4-null mice ($NOX4^{-/-}$) were exposed to LSS for 15 min and harvested and FAK and eNOS phosphorylation was analyzed by immunoblot (representative result is shown on the left). Bar graphs represent the mean ± SEM of densitometric quantifications from three independent experiments after normalization to control conditions (WT, no LSS), $^{*}p<0.05$ vs WT control. (C) WT and $NOX4^{-/-}$ mice were anesthetized and perfused with saline solution. The descending portion of the thoracic aorta was dissected. Images from aortas incubated en face with dimedone-B and anti-PECAM1 to select endothelial staining are shown ($n=8$ or 9). White arrows indicate the muscular layer without PECAM1 or dimedone-B signal and perpendicular orientation of the nuclei compared to endothelial layer. Bar graph on the right represents quantification of the dimedone-B signal from 20 regions of interest per image and three images per aorta after normalization to WT, $^{*}p<0.05$ vs WT. (D) Blot depicts a representative result of protein levels of phospho and total eNOS from MLECs isolated from WT or $NOX4^{-/-}$ mice. Bar graph on the right represents densitometric quantification of five experiments, mean ± SEM after correction by total eNOS protein content and normalized to WT samples (n=5), $^{*}p<0.05$ vs WT.

glutathione. Indeed, the proximity of a peroxide source, such as NOX2, to SHP2 significantly favors its sulfenylation after formation of a complex with the EGF receptor as recently reported [56]. It is conceivable that NOX4 could operate in the vicinity of SHP2 under LSS, thus promoting its sulfenylation in a similar fashion. Although our work did not identify the specific peptide including Cys459 of SHP2, which is considered the catalytic one [57], presumably owing to the low protein coverage and the low fragmentation/identification efficiency of biotinylated peptides, it is highly likely that this is the residue involved given its previously reported role as a target for peroxide-induced sulfenylation [15,57]. Importantly, other limitations of this work are related to the difficulty of providing the precise stoichiometry of SHP2 sulfenylation under LSS. Aside from its transient nature, sulfenylation is an oxidative modification that only recently has been approached from a quantitative standpoint [58,59]. Emerging methodologies

involving photolytic cleavage of biotin from the sulfenylated cysteines tagged with a cell-permeative alkyne dimedone analog [60] may potentially allow us to perform quantitative analysis of the sulfenylated proteome.

The NOX family of enzymes has been the object of increasing attention in the cardiovascular field in recent years [11,61–63]. In particular, several studies have highlighted the potential protective and vasodilatory role of NOX4 [8,12,64]. Results herein reported add a new angle to this notion by demonstrating its requirement for LSS-induced redox-dependent SHP2 sulfenylation and downstream FAK–eNOS activation. Previous studies have documented the interaction of SHP2 and FAK, by which inactivation of SHP2 eventually leads to FAK phosphorylation and activation [65]. Furthermore, the participation of SHP2 in the signalosome associated with fluid shear stress-dependent activation of eNOS has been previously reported, as well as the capacity of peroxide to inactivate SHP2 in endothelial cells [66]. LSS-mediated inactivation of SHP2 has been also described to be dependent on its catalytic cysteine [67]. Additionally, SHP2 can act as a protein adaptor independent of the phosphatase activity, even in the presence of high concentrations of H_2O_2, thus adding to the complexity of the role of this protein in signaling cascades [68]. FAK has been reported to be critical in the pathway leading to flow-induced coronary vasodilatation [45]. We now describe a mechanism of flow-related FAK activation of eNOS that involves previous inactivation of an upstream tyrosine phosphatase, SHP2. However, the causative link between SHP2 sulfenylation and FAK activation remains to be approached in further work. The role of NOX4 in vascular function has gained increasing attention during the past years. Nevertheless although we are unaware of studies formally testing the role of NOX4 in flow-mediated vasodilatation using loss-of-function approaches, the prevailing concept is that of NOX4-mediated vascular and endothelial protection. For example, Schröder et al. [11] demonstrated that NOX4 deficiency promotes inflammation and endothelial dysfunction. Furthermore, Ray et al. [12] reported that transgenic mice overexpressing NOX4 presented enhanced endothelium-dependent relaxation. Finally, studies in endothelial-specific transgenic NOX4 mice showed a catalase-sensitive increase in eNOS serine 1177 phosphorylation and a reduction in angiotensin II-induced contraction in mouse aorta [69]. Our data are consistent with a model in which LSS activates NOX4-dependent ROS generation promoting subsequent SHP2 oxidation by sulfenylation and downstream FAK and eNOS phosphorylation and activation (please see graphical abstract). This eNOS regulation is in accordance with results in which NOX4 transgenic mice presented increased activation of eNOS and improved vascular function against hypertensive stimuli [12]. However, although the predominant presence of NOX4 versus other isoforms in BAECs and the data related to loss of function of this enzyme herein presented strongly support its role in peroxide production after LSS, we cannot completely exclude the participation of other NOXs [70]. Of interest, in experiments performed in endothelial cells to verify the contribution of NOX1, NOX2, and NOX4 to LSS-induced redox-mediated signaling, only the deficiency of NOX4 proved to be involved [76]. However, the fact that these experiments and those depicted in Fig. 5 supporting the role of NOX4 in flow-mediated vasodilation were done in MLECs, an endothelial cell type arising from a different vascular bed and from a different species, should always be kept in mind. The use of microvasculature from null mice to study the effects observed in macrovasculature has been reported previously by us and others [8,71–73]. The combination in the same study of BAECs and in vivo endothelial experiments has been also reported [74,75]. Hence, we believe that, even though caution should always preside interpretation when different endothelial models are used, several data argue in favor of the use of MLECs as a means to test in genetic models the validity of results obtained in other endothelial cell types in culture.

The present work is the first report to our knowledge to demonstrate SHP2 cysteine sulfenylation in the endothelium under LSS. Studies performed in the whole vascular wall are consistent with protein oxidation only within the endothelial layer, supporting the role of redox regulation in this cell type. However, further studies will be needed to specifically map the topology of these signaling interactions in vascular endothelial cells.

Acknowledgments

We are indebted to Eva Blanco and Macarena Quesada for excellent technical support. We thank the laboratory of Dr. Leslie Poole for their advice on dimedone-B handling and processing. This work was supported by grants from the Ministerio de Economía y Competitividad, SAF 2012-31338 (S.L.), CSD 2007-00020 (S.L.), SAF 2010-37926 (J.V.); Instituto de Salud Carlos III, REDinREN RD12/0021/0009 (S.L.), ProteoRed-PT13/0001/0017 (J.V.), RETIC-RD12/0042/0056 (J.V.); Deutsche Forschungsgemeinschaft (SFB815/TP1 to K.S. and R.P.B. and SCHR1241/1-1 to K.S.); German Center for Cardiovascular Research; Comunidad de Madrid "Fibroteam" S2010/BMD-2321 (S.L.); and Fundación Renal "Iñigo Alvarez de Toledo" (S.L.). This work was also supported by European Cooperation in Science and Technology actions BM-1203 (EU-ROS) and BM-1005 (ENOGAS) (S.L.). A.M.S. is supported by the British Heart Foundation. The CBMSO receives institutional support from Fundación "Ramón Areces."

Appendix A. Supplementary Information

Supplementary data associated with this article can be found in the online version at. http://dx.doi.org/10.1016/j.freeradbiomed.2015.08.014.

References

[1] C. Hahn, M.A. Schwartz, Mechanotransduction in vascular physiology and atherogenesis, Nat. Rev. Mol. Cell Biol. 10 (2009) 53–62.
[2] R.E. Feaver, B.D. Gelfand, B.R. Blackman, Human haemodynamic frequency harmonics regulate the inflammatory phenotype of vascular endothelial cells, Nat. Commun. 4 (2013) 1525.
[3] E. Tzima, M. Irani-Tehrani, W.B. Kiosses, E. Dejana, D.A. Schultz, B. Engelhardt, G. Cao, H. DeLisser, M.A. Schwartz, A mechanosensory complex that mediates the endothelial cell response to fluid shear stress, Nature 437 (2005) 426–431.
[4] S. Lehoux, Redox signalling in vascular responses to shear and stretch, Cardiovasc. Res. 71 (2006) 269–279.
[5] Y. Liu, A.H. Bubolz, S. Mendoza, D.X. Zhang, D.D. Gutterman, H_2O_2 is the transferrable factor mediating flow-induced dilation in human coronary arterioles, Circ. Res. 108 (2011) 566–573.
[6] J.R. Burgoyne, M. Madhani, F. Cuello, R.L. Charles, J.P. Brennan, E. Schroder, D. D. Browning, P. Eaton, Cysteine redox sensor in PKGIa enables oxidant-induced activation, Science 317 (2007) 1393–1397.
[7] R. Breton-Romero, R. Acin-Perez, F. Rodriguez-Pascual, M. Martinez-Molledo, R.P. Brandes, E. Rial, J.A. Enriquez, S. Lamas, Laminar shear stress regulates mitochondrial dynamics, bioenergetics responses and PRX3 activation in endothelial cells, Biochim. Biophys. Acta 1843 (2014) 2403–2413.
[8] R. Breton-Romero, C. Gonzalez de Orduna, N. Romero, F.J. Sanchez-Gomez, C. de Alvaro, A. Porras, F. Rodriguez-Pascual, J. Laranjinha, R. Radi, S. Lamas, Critical role of hydrogen peroxide signaling in the sequential activation of p38 MAPK and eNOS in laminar shear stress, Free Radic. Biol. Med. 52 (2012) 1093–1100.
[9] G.W. De Keulenaer, D.C. Chappell, N. Ishizaka, R.M. Nerem, R.W. Alexander, K. K. Griendling, Oscillatory and steady laminar shear stress differentially affect human endothelial redox state: role of a superoxide-producing NADH oxidase, Circ. Res. 82 (1998) 1094–1101.
[10] U. Bayraktutan, L. Blayney, A.M. Shah, Molecular characterization and localization of the NAD(P)H oxidase components gp91-phox and p22-phox in endothelial cells, Arterioscler. Thromb. Vasc. Biol. 20 (2000) 1903–1911.
[11] K. Schröder, M. Zhang, S. Benkhoff, A. Mieth, R. Pliquett, J. Kosowski, C. Kruse,

P. Luedike, U.R. Michaelis, N. Weissmann, S. Dimmeler, A.M. Shah, R.P. Brandes, Nox4 is a protective reactive oxygen species generating vascular NADPH oxidase, Circ. Res. 110 (2012) 1217–1225.
[12] R. Ray, C.E. Murdoch, M. Wang, C.X. Santos, M. Zhang, S. Alom-Ruiz, N. Anilkumar, A. Ouattara, A.C. Cave, S.J. Walker, D.J. Grieve, R.L. Charles, P. Eaton, A.C. Brewer, A.M. Shah, Endothelial Nox4 NADPH oxidase enhances vasodilatation and reduces blood pressure in vivo, Arterioscler. Thromb. Vasc. Biol. 31 (2011) 1368–1376.
[13] A. Bindoli, J.M. Fukuto, H.J. Forman, Thiol chemistry in peroxidase catalysis and redox signaling, Antioxid. Redox Signaling 10 (2008) 1549–1564.
[14] C.C. Winterbourn, M.B. Hampton, Thiol chemistry and specificity in redox signaling, Free Radic. Biol. Med. 45 (2008) 549–561.
[15] M. Lo Conte, K.S. Carroll, The redox biochemistry of protein sulfenylation and sulfinylation, J. Biol. Chem. 288 (2013) 26480–26488.
[16] H.A. Woo, S.H. Yim, D.H. Shin, D. Kang, D.Y. Yu, S.G. Rhee, Inactivation of peroxiredoxin I by phosphorylation allows localized H(2)O(2) accumulation for cell signaling, Cell 140 (2010) 517–528.
[17] C. Klomsiri, K.J. Nelson, E. Bechtold, L. Soito, L.C. Johnson, W.T. Lowther, S. E. Ryu, S.B. King, C.M. Furdui, L.B. Poole, Use of dimedone-based chemical probes for sulfenic acid detection evaluation of conditions affecting probe incorporation into redox-sensitive proteins, Methods Enzymol 473 (2010) 77–94.
[18] K.J. Nelson, C. Klomsiri, S.G. Codreanu, L. Soito, D.C. Liebler, L.C. Rogers, L. W. Daniel, L.B. Poole, Use of dimedone-based chemical probes for sulfenic acid detection methods to visualize and identify labeled proteins, Methods Enzymol 473 (2010) 95–115.
[19] M. Zhang, A.C. Brewer, K. Schroder, C.X. Santos, D.J. Grieve, M. Wang, N. Anilkumar, B. Yu, X. Dong, S.J. Walker, R.P. Brandes, A.M. Shah, NADPH oxidase-4 mediates protection against chronic load-induced stress in mouse hearts by enhancing angiogenesis, Proc. Natl. Acad. Sci. USA 107 (2010) 18121–18126.
[20] S. Lamas, P.A. Marsden, G.K. Li, P. Tempst, T. Michel, Endothelial nitric oxide synthase: molecular cloning and characterization of a distinct constitutive enzyme isoform, Proc. Natl. Acad. Sci. USA 89 (1992) 6348–6352.
[21] I. Fleming, J. Bauersachs, B. Fisslthaler, R. Busse, Ca^{2+}-independent activation of the endothelial nitric oxide synthase in response to tyrosine phosphatase inhibitors and fluid shear stress, Circ. Res. 82 (1998) 686–695.
[22] H. Zhao, J. Joseph, H.M. Fales, E.A. Sokoloski, R.L. Levine, J. Vasquez-Vivar, B. Kalyanaraman, Detection and characterization of the product of hydroethidine and intracellular superoxide by HPLC and limitations of fluorescence, Proc. Natl. Acad. Sci. USA 102 (2005) 5727–5732.
[23] V.V. Belousov, A.F. Fradkov, K.A. Lukyanov, D.B. Staroverov, K.S. Shakhbazov, A. V. Terskikh, S. Lukyanov, Genetically encoded fluorescent indicator for intracellular hydrogen peroxide, Nat. Methods 3 (2006) 281–286.
[24] N. Anilkumar, R. Weber, M. Zhang, A. Brewer, A.M. Shah, Nox4 and Nox2 NADPH oxidases mediate distinct cellular redox signaling responses to agonist stimulation, Arterioscler. Thromb. Vasc. Biol. 28 (2008) 1347–1354.
[25] E. Bonzon-Kulichenko, D. Perez-Hernandez, E. Nunez, P. Martinez-Acedo, P. Navarro, M. Trevisan-Herraz, C. Ramos Mdel, S. Sierra, S. Martinez-Martinez, M. Ruiz-Meana, E. Miro-Casas, D. Garcia-Dorado, J.M. Redondo, J.S. Burgos, J. Vazquez, A robust method for quantitative high-throughput analysis of proteomes by ^{18}O labeling, Mol. Cell. Proteomics 10 (M110) (2011) 003335.
[26] P. Martinez-Acedo, E. Nunez, F.J. Gomez, M. Moreno, E. Ramos, A. Izquierdo-Alvarez, E. Miro-Casas, R. Mesa, P. Rodriguez, A. Martinez-Ruiz, D.G. Dorado, S. Lamas, J. Vazquez, A novel strategy for global analysis of the dynamic thiol redox proteome, Mol. Cell. Proteomics 11 (2012) 800–813.
[27] S. Martinez-Bartolome, P. Navarro, F. Martin-Maroto, D. Lopez-Ferrer, A. Ramos-Fernandez, M. Villar, J.P. Garcia-Ruiz, J. Vazquez, Properties of average score distributions of SEQUEST: the probability ratio method, Mol. Cell. Proteomics 7 (2008) 1135–1145.
[28] P. Navarro, J. Vazquez, A refined method to calculate false discovery rates for peptide identification using decoy databases, J. Proteome Res. 8 (2009) 1792–1796.
[29] S.I. Dikalov, A.E. Dikalova, A.T. Bikineyeva, H.H. Schmidt, D.G. Harrison, K. K. Griendling, Distinct roles of Nox1 and Nox4 in basal and angiotensin II-stimulated superoxide and hydrogen peroxide production, Free Radic. Biol. Med. 45 (2008) 1340–1351.
[30] P. Hernansanz-Agustin, A. Izquierdo-Alvarez, F.J. Sanchez-Gomez, E. Ramos, T. Villa-Pina, S. Lamas, A. Bogdanova, A. Martinez-Ruiz, Acute hypoxia produces a superoxide burst in cells, Free Radic. Biol. Med. 71 (2014) 146–156.
[31] M. Redondo-Horcajo, N. Romero, P. Martinez-Acedo, A. Martinez-Ruiz, C. Quijano, C.F. Lourenco, N. Movilla, J.A. Enriquez, F. Rodriguez-Pascual, E. Rial, R. Radi, J. Vazquez, S. Lamas, Cyclosporine A-induced nitration of tyrosine 34 MnSOD in endothelial cells: role of mitochondrial superoxide, Cardiovasc. Res. 87 (2010) 356–365.
[32] Y.M. Janssen-Heininger, B.T. Mossman, N.H. Heintz, H.J. Forman, B. Kalyanaraman, T. Finkel, J.S. Stamler, S.G. Rhee, A. van der Vliet, Redox-based regulation of signal transduction: principles, pitfalls, and promises, Free Radic. Biol. Med. 45 (2008) 1–17.
[33] S.G. Rhee, T.S. Chang, W. Jeong, D. Kang, Methods for detection and measurement of hydrogen peroxide inside and outside of cells, Mol. Cells 29 (2010) 539–549.
[34] H.J. Forman, O. Augusto, R. Brigelius-Flohe, P.A. Dennery, B. Kalyanaraman, H. Ischiropoulos, G.E. Mann, R. Radi, L.J. Roberts 2nd, J. Vina, K.J. Davies, Even free radicals should follow some rules: a guide to free radical research terminology and methodology, Free Radic. Biol. Med. 78 (2015) 233–235.
[35] J. Weller, K.M. Kizina, K. Can, G. Bao, M. Muller, Response properties of the genetically encoded optical H_2O_2 sensor HyPer, Free Radic. Biol. Med. 76 (2014) 227–241.
[36] R.C. Ziegelstein, L. Cheng, M.C. Capogrossi, Flow-dependent cytosolic acidification of vascular endothelial cells, Science 258 (1992) 656–659.
[37] I. Takac, K. Schroder, L. Zhang, B. Lardy, N. Anilkumar, J.D. Lambeth, A.M. Shah, F. Morel, R.P. Brandes, The E-loop is involved in hydrogen peroxide formation by the NADPH oxidase Nox4, J. Biol. Chem. 286 (2011) 13304–13313.
[38] J.M. Denu, K.G. Tanner, Specific and reversible inactivation of protein tyrosine phosphatases by hydrogen peroxide: evidence for a sulfenic acid intermediate and implications for redox regulation, Biochemistry 37 (1998) 5633–5642.
[39] Y.W. Lou, Y.Y. Chen, S.F. Hsu, R.K. Chen, C.L. Lee, K.H. Khoo, N.K. Tonks, T. C. Meng, Redox regulation of the protein tyrosine phosphatase PTP1B in cancer cells, FEBS J. 275 (2008) 69–88.
[40] A. Salmeen, J.N. Andersen, M.P. Myers, T.C. Meng, J.A. Hinks, N.K. Tonks, D. Barford, Redox regulation of protein tyrosine phosphatase 1B involves a sulphenyl-amide intermediate, Nature 423 (2003) 769–773.
[41] R.L. van Montfort, M. Congreve, D. Tisi, R. Carr, H. Jhoti, Oxidation state of the active-site cysteine in protein tyrosine phosphatase 1B, Nature 423 (2003) 773–777.
[42] T.C. Meng, D.A. Buckley, S. Galic, T. Tiganis, N.K. Tonks, Regulation of insulin signaling through reversible oxidation of the protein-tyrosine phosphatases TC45 and PTP1B, J. Biol. Chem. 279 (2004) 37716–37725.
[43] Z.R. Hartman, M.D. Schaller, Y.M. Agazie, The tyrosine phosphatase SHP2 regulates focal adhesion kinase to promote EGF-induced lamellipodia persistence and cell migration, Mol. Cancer Res. 11 (2013) 651–664.
[44] H. Miao, E. Burnett, M. Kinch, E. Simon, B. Wang, Activation of EphA2 kinase suppresses integrin function and causes focal-adhesion-kinase dephosphorylation, Nat. Cell Biol. 2 (2000) 62–69.
[45] R. Koshida, P. Rocic, S. Saito, T. Kiyooka, C. Zhang, W.M. Chilian, Role of focal adhesion kinase in flow-induced dilation of coronary arterioles, Arterioscler. Thromb. Vasc. Biol. 25 (2005) 2548–2553.
[46] G.B. Atkins, Y. Wang, G.H. Mahabeleshwar, H. Shi, H. Gao, D. Kawanami, V. Natesan, Z. Lin, D.I. Simon, M.K. Jain, Hemizygous deficiency of Kruppel-like factor 2 augments experimental atherosclerosis, Circ. Res. 103 (2008) 690–693.
[47] L. Hajra, A.I. Evans, M. Chen, S.J. Hyduk, T. Collins, M.I. Cybulsky, The NF-kappa B signal transduction pathway in aortic endothelial cells is primed for activation in regions predisposed to atherosclerotic lesion formation, Proc. Natl. Acad. Sci. USA 97 (2000) 9052–9057.
[48] R.P. Brandes, F.H. Schmitz-Winnenthal, M. Feletou, A. Godecke, P.L. Huang, P. M. Vanhoutte, I. Fleming, R. Busse, An endothelium-derived hyperpolarizing factor distinct from NO and prostacyclin is a major endothelium-dependent vasodilator in resistance vessels of wild-type and endothelial NO synthase knockout mice, Proc. Natl. Acad. Sci. USA 97 (2000) 9747–9752.
[49] O. Prysyazhna, O. Rudyk, P. Eaton, Single atom substitution in mouse protein kinase G eliminates oxidant sensing to cause hypertension, Nat. Med 18 (2012) 286–290.
[50] D.X. Zhang, L. Borbouse, D. Gebremedhin, S.A. Mendoza, N.S. Zinkevich, R. Li, D.D. Gutterman, H_2O_2-induced dilation in human coronary arterioles: role of protein kinase G dimerization and large-conductance Ca^{2+}-activated K^+ channel activation, Circ. Res. 110 (2012) 471–480.
[51] D. Barford, A.J. Flint, N.K. Tonks, Crystal structure of human protein tyrosine phosphatase 1B, Science 263 (1994) 1397–1404.
[52] A. Salmeen, D. Barford, Functions and mechanisms of redox regulation of cysteine-based phosphatases, Antioxid. Redox Signaling 7 (2005) 560–577.
[53] B. Boivin, S. Zhang, J.L. Arbiser, Z.Y. Zhang, N.K. Tonks, A modified cysteinyl-labeling assay reveals reversible oxidation of protein tyrosine phosphatases in angiomyolipoma cells, Proc. Natl. Acad. Sci. USA 105 (2008) 9959–9964.
[54] J.C. Juarez, M. Manuia, M.E. Burnett, O. Betancourt, B. Boivin, D.E. Shaw, N. K. Tonks, A.P. Mazar, F. Donate, Superoxide dismutase 1 (SOD1) is essential for H_2O_2-mediated oxidation and inactivation of phosphatases in growth factor signaling, Proc. Natl. Acad. Sci. USA 105 (2008) 7147–7152.
[55] C.C. Winterbourn, Reconciling the chemistry and biology of reactive oxygen species, Nat. Chem. Biol. 4 (2008) 278–286.
[56] C.E. Paulsen, T.H. Truong, F.J. Garcia, A. Homann, V. Gupta, S.E. Leonard, K. S. Carroll, Peroxide-dependent sulfenylation of the EGFR catalytic site enhances kinase activity, Nat. Chem. Biol. 8 (2011) 57–64.
[57] C.Y. Chen, D. Willard, J. Rudolph, Redox regulation of SH2-domain-containing protein tyrosine phosphatases by two backdoor cysteines, Biochemistry 48 (2009) 1399–1409.
[58] V. Gupta, K.S. Carroll, Sulfenic acid chemistry, detection and cellular lifetime, Biochim. Biophys. Acta 1840 (2014) 847–875.
[59] C.E. Paulsen, K.S. Carroll, Cysteine-mediated redox signaling: chemistry, biology, and tools for discovery, Chem. Rev. 113 (2013) 4633–4679.
[60] J. Yang, V. Gupta, K.A. Tallman, N.A. Porter, K.S. Carroll, D.C. Liebler, Global, in situ, site-specific analysis of protein S-sulfenylation, Nat. Protoc. 10 (2015) 1022–1037.
[61] R.P. Brandes, N. Weissmann, K. Schroder, Nox family NADPH oxidases in mechano-transduction: mechanisms and consequences, Antioxid. Redox Signaling 20 (2013) 887–898.
[62] B. Lassegue, A. San Martin, K.K. Griendling, Biochemistry, physiology, and pathophysiology of NADPH oxidases in the cardiovascular system, Circ. Res. 110 (2012) 1364–1390.
[63] A. Sirker, M. Zhang, A.M. Shah, NADPH oxidases in cardiovascular disease: insights from in vivo models and clinical studies, Basic Res. Cardiol. 106 (2011)

735–747.
[64] A. Babelova, D. Avaniadi, O. Jung, C. Fork, J. Beckmann, J. Kosowski, N. Weissmann, N. Anilkumar, A.M. Shah, L. Schaefer, K. Schroder, R.P. Brandes, Role of Nox4 in murine models of kidney disease, Free Radic. Biol. Med. 53 (2012) 842–853.
[65] R. Tsutsumi, A. Takahashi, T. Azuma, H. Higashi, M. Hatakeyama, Focal adhesion kinase is a substrate and downstream effector of SHP-2 complexed with Helicobacter pylori CagA, Mol. Cell. Biol. 26 (2006) 261–276.
[66] H. Tang, Q. Hao, S.A. Rutherford, B. Low, Z.J. Zhao, Inactivation of SRC family tyrosine kinases by reactive oxygen species in vivo, J. Biol. Chem. 280 (2005) 23918–23925.
[67] N. Lerner-Marmarosh, M. Yoshizumi, W. Che, J. Surapisitchat, H. Kawakatsu, M. Akaike, B. Ding, Q. Huang, C. Yan, B.C. Berk, J. Abe, Inhibition of tumor necrosis factor-[alpha]-induced SHP-2 phosphatase activity by shear stress: a mechanism to reduce endothelial inflammation, Arterioscler. Thromb. Vasc. Biol. 23 (2003) 1775–1781.
[68] A. Jo, H. Park, S.H. Lee, S.H. Ahn, H.J. Kim, E.M. Park, Y.H. Choi, SHP-2 binds to caveolin-1 and regulates Src activity via competitive inhibition of CSK in response to H_2O_2 in astrocytes, PLoS One 9 (2014) e91582.
[69] S.M. Craige, K. Chen, Y. Pei, C. Li, X. Huang, C. Chen, R. Shibata, K. Sato, K. Walsh, J.F. Keaney Jr., NADPH oxidase 4 promotes endothelial angiogenesis through endothelial nitric oxide synthase activation, Circulation 124 (2011) 731–740.
[70] R.P. Brandes, N. Weissmann, K. Schroder, Nox family NADPH oxidases: molecular mechanisms of activation, Free Radic. Biol. Med. 76 (2014) 208–226.
[71] S. Borniquel, N. Garcia-Quintans, I. Valle, Y. Olmos, B. Wild, F. Martinez-Granero, E. Soria, S. Lamas, M. Monsalve, Inactivation of Foxo3a and subsequent downregulation of PGC-1 alpha mediate nitric oxide-induced endothelial cell migration, Mol. Cell. Biol. 30 (2010) 4035–4044.
[72] Y. Olmos, F.J. Sanchez-Gomez, B. Wild, N. Garcia-Quintans, S. Cabezudo, S. Lamas, M. Monsalve, SirT1 regulation of antioxidant genes is dependent on the formation of a FoxO3a/PGC-1alpha complex, Antioxid. Redox Signaling 19 (2013) 1507–1521.
[73] B.E. Sumpio, S. Yun, A.C. Cordova, M. Haga, J. Zhang, Y. Koh, J.A. Madri, MAPKs (ERK1/2, p38) and AKT can be phosphorylated by shear stress independently of platelet endothelial cell adhesion molecule-1 (CD31) in vascular endothelial cells, J. Biol. Chem. 280 (2005) 11185–11191.
[74] F. De Marchis, D. Ribatti, C. Giampietri, A. Lentini, D. Faraone, M. Scoccianti, M. C. Capogrossi, A. Facchiano, Platelet-derived growth factor inhibits basic fibroblast growth factor angiogenic properties in vitro and in vivo through its alpha receptor, Blood 99 (2002) 2045–2053.
[75] N. Weiss, Y.Y. Zhang, S. Heydrick, C. Bierl, J. Loscalzo, Overexpression of cellular glutathione peroxidase rescues homocyst(e)ine-induced endothelial dysfunction, Proc. Natl. Acad. Sci. USA 98 (2001) 12503–12508.
[76] R. Bretón-Romero, Redox signaling responses to laminar shear stress in vascular endothelial cells [Ph.D. dissertation]. Universidad Autónoma de Madrid, 21 June, 2013.